J Mater Sci (2009) 44:601–607
DOI 10.1007/s10853-008-3080-5

In situ TEM study of Au–Cu alloy nanoparticle migration and coalescence

Abhay Raj S. Gautam · James M. Howe

Received: 6 May 2008 / Accepted: 21 October 2008 / Published online: 10 November 2008

Abstract The diffusion and coalescence of Au–Cu alloy nanoparticles was studied at high magnification using in situ transmission electron microscopy. The particles prepared by physical vapor deposition onto amorphous-C support films had an average composition of Cu–43 at% Au and diameters of 15–50 nm. In the case analyzed, the larger of two nanoparticles remained stationary throughout the coalescence process while a smaller nanoparticle moved toward the larger particle at a temperature of ~573 K. The surface of the small nanoparticle was observed to fluctuate while approaching the larger particle, demonstrating that collective atom process occurs along the particle periphery. The particle also decreased in size during the process, indicating that it was losing mass as well as migrating. Direct evidence of a diffusional flux between particles was observed before the coalescence process. The small nanoparticle coalesced into the large one at a highly accelerated rate compared to its prior migration.

Introduction

The dynamic behavior of nanoparticles or clusters of atoms is of interest to many fields including micro-electronics, optoelectronics, and catalysis [1]. Some of these applications such as catalysis try to avoid the coalescence or agglomeration of nanoparticles, while others desire better control over the coarsening process such as for thin-film structures. To achieve either of these objectives, it is imperative to understand the mechanisms involved in the process of coarsening.

Substantial work has been done to study coarsening processes in various environments. The thermodynamic framework used to explain this phenomenon was first developed by Ostwald to explain grain coarsening in solutions. Particles in a matrix try to maintain local thermodynamic equilibrium with their surroundings. Smaller particles are associated with a higher chemical potential compared to larger particles due to their smaller radius of curvature. This sets up a chemical potential difference in three-dimensions (3D), resulting in a diffusional flux from small particles to larger particles [2]. This phenomenon has been studied in detail for grain and precipitate coarsening, which involve 3D diffusion of atomic species [3]. Extension of this phenomenon is applicable to the process of coarsening of particles on a substrate [4, 5]. The difference being that instead of trying to maintain equilibrium in three-dimensions the particles try to attain local thermodynamic equilibrium with the two-dimensional gas on the surface of the substrate. This equilibrium is given by the Gibbs-Thomson equation according to which smaller particles have higher vapor pressure due to their smaller radius of curvature. This results in a higher number of free atoms (2D gas) on the substrate in the vicinity of small particles compared to large particle, which sets up a composition gradient leading to 2D diffusion of atoms from smaller particles to larger particles [6].

Another mechanism responsible for the coarsening of particles is the migration of atomic clusters, or nanoparticles, on the substrate [7]. Cluster migration has been found to be the prominent coarsening mechanism in the case of

A. R. S. Gautam (✉) · J. M. Howe
Department of Materials Science and Engineering,
University of Virginia, Charlottesville, VA 22904-4745, USA
e-mail: arg5b@virginia.edu

J. M. Howe
e-mail: jh9s@virginia.edu

small nanoparticles. One possible mechanism responsible for particle motion has been reported to be adatom diffusion (evaporation–condensation), which involves random exchange of atoms between the edge of the particle and surrounding 2D atomic gas, accompanied by condensation of atoms at other parts of the particle. This asymmetric evaporation and condensation of atoms leads to motion of the center of mass of the particle [8]. Another mechanism involves collective vibrational motion of the atoms constituting the particle. This mechanism involves synchronization of the atomic vibrations of the particle that results in motion of the cluster as a whole [9, 10]. Along similar lines, in situ transmission electron microscope (TEM) studies have shown that metal nanoparticles may fluctuate among various metastable structural states when exposed to intense electron irradiation [11, 12].

It is usually observed that the particle trajectory during migration is random Brownian motion [13]. This is often the case when the inter-particle separation is larger than the diameter of the particle. Based on this observation, atomic clusters are considered as non-interacting particles. However, experimental observations suggest that particles do have some field of attractive nature and one possible mechanism for such a field could be the growth/decay flow of edges due to the composition profile around the particles [14]. In work involving simulation of particle kinetics, the models usually do not consider any interaction between the particles, although the effect of attractive and repulsive interactions between particles has been explored in a few cases [15]. This interaction was incorporated using a cut-off-distance based force-field between the particles, above which the particles do not interact with each other and move according to random Brownian motion.

The process of coalescence is usually assumed to occur as soon as particles come into contact with one other. The assumption of immediate coalescence will not affect the evolution of the final quasi-equilibrium structure or distribution of particles, but it will affect kinetic aspects of the process. In addition, there is evidence that this assumption is not physically correct in certain situations. For example, computational studies of particle coalescence suggest that during the initial stages, the process involves the formation of low-energy interface between the particles. This low-energy configuration is achieved by elastic and plastic deformations along with particle rotation [16].

In this paper we observe the migration and coalescence of a relatively large Au–Cu nanoparticle ($\sim$15 nm in diameter) at high magnification using in situ TEM. The present work is a derivative of an ongoing study on the dynamic behavior of order–disorder interfaces in Au–Cu nanoparticles. Gold–copper alloy is a model system to carry out such in situ TEM experiments because of the low critical temperature and negligible solubility of both Au and Cu in the amorphous carbon film and vice versa [17, 18]. In this paper, we present the dynamic behavior of the particle ($\sim$15 nm in diameter) on an amorphous carbon substrate supported on a Mo grid, as it interacts with the nearest larger particle ($\sim$45 nm in diameter) located 11 nm away.

Experimental procedure

Au–Cu alloy nanoparticles were prepared by vapor deposition as described in detail elsewhere [19]. In brief, high-purity Au and Cu metals were evaporated from W baskets on to heated amorphous-C substrates under vacuum. The amorphous-C film had a manufacturer-reported thickness of $\sim$20 nm and was supported on Mo-mesh TEM grids. The deposition was performed with a substrate temperature of 906 K and a base pressure of 2×10^{-8} Torr. The samples were annealed at 906 K for 3 h followed by cooling to room temperature under vacuum. In situ heating experiments were performed in a JEOL 2010F analytical microscope using a Gatan® double-tilt water-cooled heating holder. The present experiment was performed at a temperature of $\sim$573 K. The average composition of the sample used in the present experiment was Cu–43 at.% Au, as determined by quantitative energy-dispersive X-ray spectroscopy in the TEM [19]. Individual particle composition was found to be within ±5% of the average composition. It has been reported that the compositional uniformity of Au–Cu alloy particles shows some size dependence for particle sizes below 10 nm, and becomes significant for particle sizes of 5 nm or less [20]. Since the particles used in this study were larger than 10 nm in diameter, we can assume that any effects of particle size on composition are negligible.

Images were recorded on a video cassette through a TV-rate CCD camera and were later digitized at 30 fps using Adobe Premier® 6.0 software and an Aurora Fuse capture card with MJPEG A compression algorithm. The individual frames from the digital video were then exported in uncompressed TIFF format. Due to the low contrast between the nanoparticles and amorphous-C substrate, it was necessary to boost the contrast by saturating the image. The "imadjust" MATLAB® function was used to improve the contrast of the images by saturating 1% of the data at the minimum and maximum intensities. In order to convert the saturated grayscale images (256 bit) to binary, approximate threshold values were determined using the "greythresh" MATLAB® function. This function utilizes Otsu's method, which selects the threshold by minimizing the interclass variance of the black and white pixels. Using this threshold value as a guide, the working threshold value was determined by trail and error. Initially, every 30th

image (1 fps) was chosen and the threshold limit was determined for each image to achieve the best possible match with the original image. Finally, using these values for the threshold, the saturated grayscale images were converted to binary using the "im2bw" MATLAB® function, which replaces all the pixels in the image with a luminance greater than the threshold with a value of 1 (white), and the others with a value of 0 (black). This procedure gave an image with white particles on a black substrate. These images were then used to quantify the surface fluctuation (radius of the particle), interparticle separation, and projected area of the small particle, using the "regionprops" function in the MATLAB Image toolbox.

Results and discussion

In order to study the details of particle migration and coalescence, a high-magnification video of a mobile nanoparticle was recorded until coalescence was complete. The sample used in present study had Au–Cu alloy particle size distribution in the range of 15 to 50 nm in diameter as shown in Fig. 1a. The size of the nanoparticle reported in this paper corresponds to the projected area of the particle in the TEM image. Fig. 1b shows a TEM image of the particle that was followed to study the coalescence dynamics. The diameter of small particle marked A was ~15 nm while that of the large particle B was ~45 nm. Several smaller (2–3 nm) particles overlapping these two particles are on the other side of the C substrate. Fig. 1c shows a schematic side view of the nanoparticles on the substrate, including their appropriate contact angles.

The larger of the two particles in Fig. 1b was observed to remain stationary at all times while the smaller particle moved toward it. Experimental studies have confirmed that particle migration and coalescence is an important coarsening mechanism for particle sizes in the range of 5 nm or smaller [21], but the occurrence of such phenomena involving particles larger than this is speculative [22]. General observation of the sample revealed that all of the mobile particles were of similar size (i.e., ~15 nm) as the one analyzed in this paper. Larger particles occasionally coalesced by changing their shape (not recorded on tape). This was observed only when two or more particles were close enough that deformation of the particles toward each other allowed for coalescence without appreciable movement of the centroid of the particles. Similar observations have been reported by Wanner et al. [23].

Figure 2a shows a binary image of the two particles after performing the procedure described in the previous section. The interparticle distance used in this paper corresponds to the distance between the center of the smaller

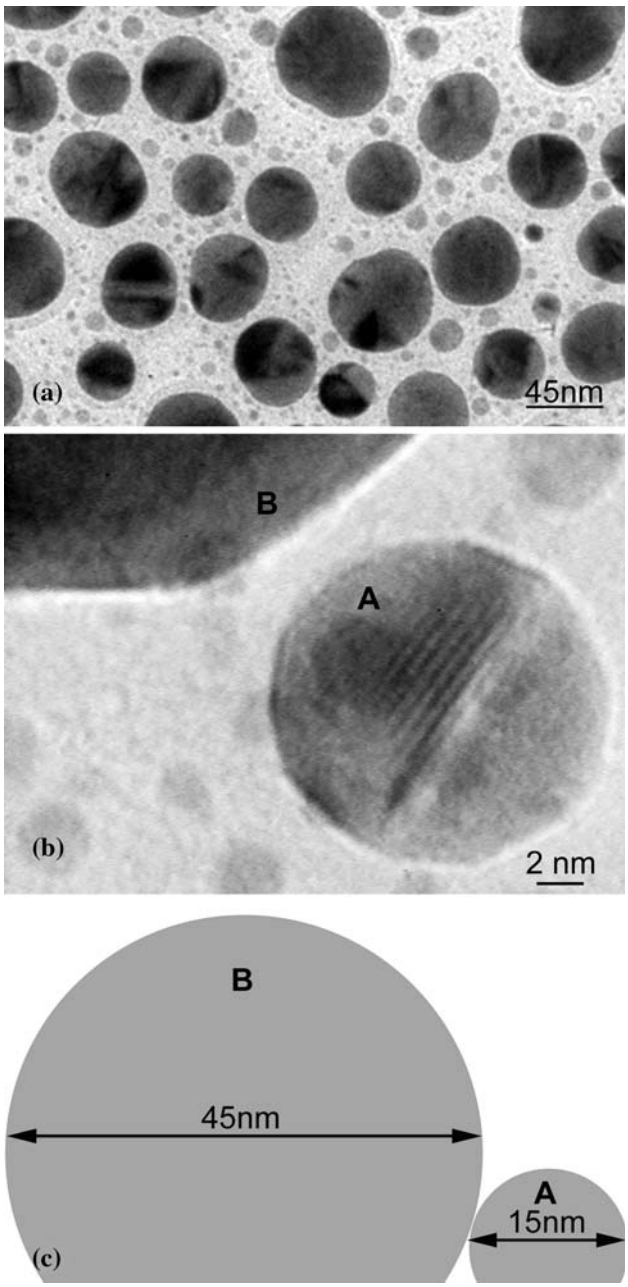

Fig. 1 **a** Distribution of Au–Cu alloy particles on the amorphous-C film. **b** The two particles studied, where the smaller one A moved toward B. **c** Schematic of the sizes and shapes of the particles on the film viewed from the side

particle and a fixed feature at the edge of the larger particle that stayed fairly stationary over the period of observation. The center of the small particle was taken to be its centroid. In addition to physical motion of the particle, other factors that can change the position of the centroid are the particle shape and size. The area and eccentricity (ratio of the major and minor axis) of the particle were measured for all the images. It was found that the area of the particle decreased by 2.5 nm^2 from an initial value of 166 nm^2 over a period

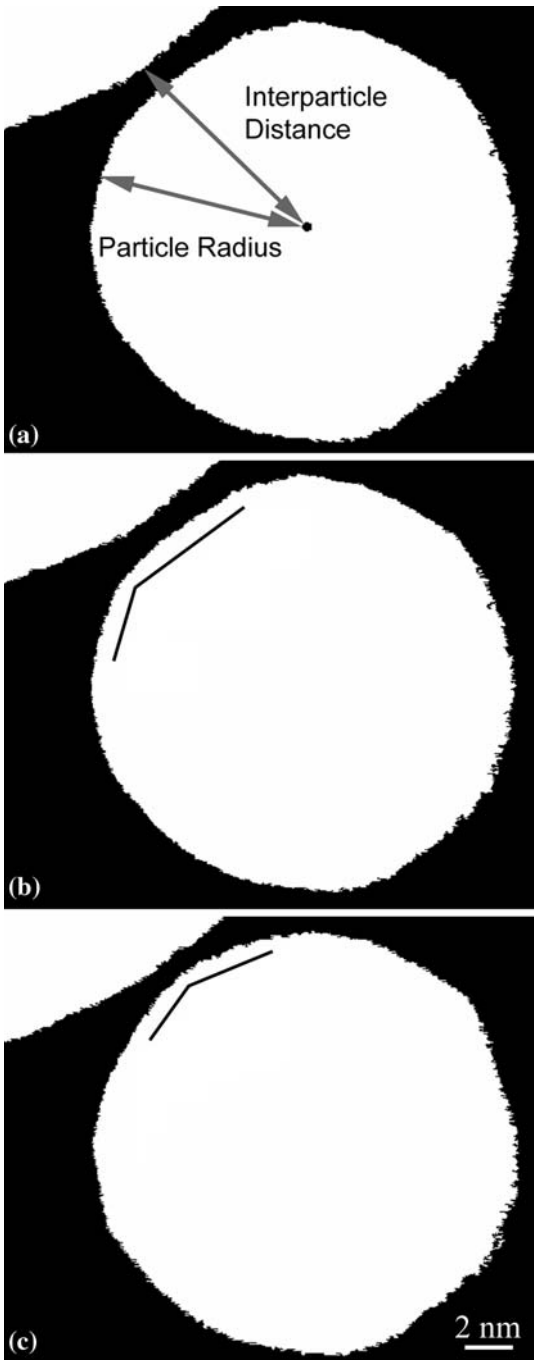

Fig. 2 **a** Binary image showing the interparticle distance and radius of the particle measured versus time. **b** and **c** show decomposition of a single facet into two facets due to surface fluctuations

of 60 s, while the eccentricity increased by 0.05 from an initial value of 1.15 over the same period. These factors affect the calculated position of the centroid, but since the changes are small relative to the initial values, their effect on the centroid position are also small compared to the magnitude of displacements being measured. In order to ensure the statistical significance of the results, one-way

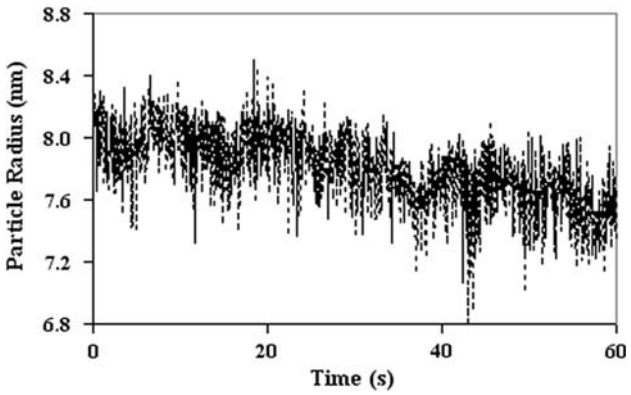

Fig. 3 The radius of the small nanoparticle versus time. The measured distance corresponds to the distance between the centroid and the edge of the particle that showed the maximum fluctuation amplitude (refer to Fig. 2a)

single-factor analysis of variance (ANOVA) was carried out on two sets of data taken 60 s apart, with each set having 30 data points (distance of small particle from the edge of the large particle). One-way ANOVA (with $F(1,58) = 8.03$, $p = 0.06$, $F_{\text{Crit}} = 4.01$, and 95% confidence interval) revealed that the position of the small particle did change over the time period with respect to the large particle.

Rearrangements of near-surface atoms leading to particle shape changes have been reported for small particles [12]. In the present work, the surface of the small particle was observed to fluctuate while approaching the larger particle. Surface fluctuations on the small particle usually involved decomposition of a single facet into two facets rather than being random in nature, as shown in Fig. 2b and c. The amplitude of fluctuation (0.5 nm), was largest for the edge closest to the large particle and occurred at a frequency of $\sim$10 times per second when the interparticle distance was 11 nm (Fig. 3). The observed fluctuations demonstrate that collective atom processes occur along the particle periphery. The occurrence of strong fluctuations along the particle periphery in the direction of particle motion indicates that this collective motion of atoms (surface fluctuation) may be contributing toward its motion. The opposite edge of the particle was also observed to fluctuate, but with smaller amplitude, while other edges showed negligible fluctuation. Thus, the fluctuations occurred asymmetrically and primarily along the direction of particle approach. Information regarding the nature of the facets would be valuable; however, in this work it was difficult to index the facets as the particle orientation was along a high-index zone axis. Any attempts to use nanobeam electron diffraction to accurately index the particle and its facets would have significantly affected the migration/coarsening process due to the high electron dose in the small probe and was thus avoided. It is worth

mentioning that the facet orientation could have a significant affect on the fluctuation amplitude, with high-energy surfaces/facets expected to exhibit higher fluctuation amplitudes than low-energy surfaces/facets.

The size of the small nanoparticle also decreased during the process of migration from 166 nm^2 to 2.5 nm^2 over a period of 60 s. Thus, the particle lost mass as it migrated toward the large particle. The error involved in this measurement is difficult to quantify due to number of steps involved; however, one-way ANOVA was carried out on two sets of data 60 s apart, each set having 10 data points (the measured area). A one-way ANOVA (with $F(1,18) = 32.35$, $p < 0.001$, $F_{crit} = 4.41$, and 95% confidence interval) revealed that the area of the particle did change over time. No perceptible change in the size of the larger particle was observed over the same period. This observation is expected given that the large particle is too big to show any appreciable change due to the addition of a comparatively small mass from the smaller particle. The decrease in size of the small nanoparticle suggests that a phenomenon similar to Ostwald ripening occurred during particle migration, where atoms from the small particle diffused toward the large particle. This flux of atoms is likely coupled to the fluctuations that occur preferentially along the closest direction between the particles.

It is difficult to measure the composition of the atomic flux without affecting the overall process; however, some inference can be drawn based on behavior of Au and Cu atoms on an amorphous-C substrate. Au and Cu have negligible solubility in C [17, 18]. Also, the interaction energies of Au and Cu with C are reported as 0.25 eV/atom and ~0.12 eV/atom, respectively [24]. From these values it can be inferred that Cu, which has a weaker interaction with C, may have a higher mobility and, therefore, may migrate more rapidly to the large particle, thereby making the flux composition slightly different. It is worth noting that any compositional difference between two particles, if favorable, could also be partially responsible for atomic diffusion toward the large particle. However, as mentioned in the experimental procedure, the maximum possible difference in the composition of the two particles would not be more than ±5 at.%, which is small enough not to have a major effect on the overall diffusion process. Hence, both of these possibilities are considered to not have a significant affect on the observed mechanisms of the process.

The trajectory of the small particle was essentially along a straight line toward the larger particle. This provides direct evidence that there is some type of interaction between the two particles that causes the smaller particle to follow the shortest path rather than approaching through random motion. The edge fluctuations and loss of mass described previously, suggest that the interaction may be through a direct diffusional flux. Most theoretical or simulation studies of cluster migration and coalescence do not incorporate such interactions among the particles. There have been some investigations to study the effect of short-range interactions between particles, wherein implementation considers attraction between particles up to a certain cutoff distance [15]. Our observations support this type of approach and agree with other experimental observations of particle interaction [14].

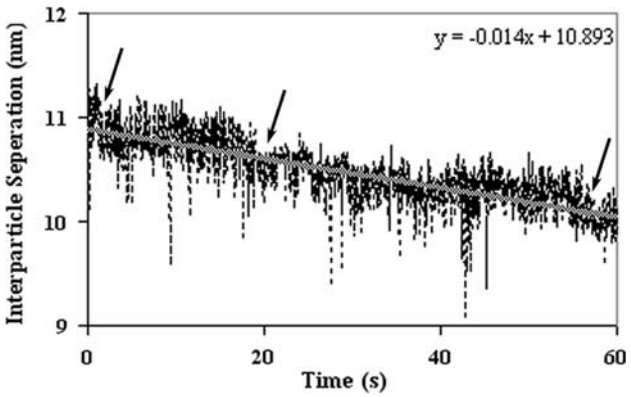

Fig. 4 Variation of interparticle distance versus time. The high-frequency fluctuations do not represent real physical phenomenon, but are due to changes in the shape, edge, and size of the particle

Figure 4 shows the position of the small particle as function of time. The slope of the linear fit represents the average velocity of migration, which was 0.014 nm/s. It appears form the plot that the velocity of the particle was not constant but changed over the period of observation; however, the change involved is small and within measurement error. As previously mentioned, the particle is losing mass while migrating. Previous analyses have shown that the migration rate of clusters is proportional to their size raised to certain power, where the value of the exponent depends upon the mechanism by which the particle migrates [13, 22]. In contrast to this, we did not observe any perceptible increase in the velocity of the particle over the time of observation although its volume decreased by only ~1.5% over a period of 60 s. If we use the approximate equation for the diffusivity of $D = d^2/4\tau$ as applied to cluster migration, where d is the particle diameter and τ the time required by the particle to diffuse the distance d, we obtain a diffusivity for the particle of the order of $\sim 10^{-17}$ cm^2/s. This small value of the diffusivity is close to values reported for the migration of smaller clusters (~5 nm diameter) in epitaxial systems. In the case of non-epitaxial systems like ours, reported values are typically of the order of $\sim 10^{-8}$ cm^2/s or less [22, 25]. One possible explanation for such a large difference could be that the size of the present particle is much larger than usually observed for theoretical studies of migration kinetics of clusters on non-epitaxial systems.

When the two particles came into contact, coalescence did not take place immediately. In fact, the particles stayed in contact for more than 15 s after impingement before fusing. Although the reason for the delay in particle coalescence is not obvious, we do not believe that it was caused by the presence of either hydrocarbon or carbon contamination layers on the particle surfaces. This is because no evidence of such layers was observed in the high-magnification images and also, because the specimen conditions, i.e., a temperature of ~573 K under a 200 keV electron beam, should be sufficient to desorb such layers. The low affinity of Au and C and the tendency of Au to segregate toward the surface in Au–Cu alloys [26] also suggest that any contamination of the particle surfaces with C should be small and have a minimal effect on their behavior.

A possible reason for the delay in coalescence could be due to the orientation of the two particles. Using molecular dynamics, Zhu and Averback [16] showed that two contacting particles try to form a low-energy interface by elastic and plastic deformations, as well as by particle rotations. No evidence of substantial particle rotation was observed in our experiments; however, the possibility of particle deformations leading to a low-energy interface, followed by liquid-like coalescence, could be a reason for the delay in coalescence. The facet fluctuations mentioned previously clearly indicate that particle deformations are occurring at the nanoscale. This delay could also be partially due to wetting of the particles, but as can be seen from Fig. 5a, the particles maintained distinct surfaces while they were in contact for more than 15 s, indicating that the coalescence process did not involve classical particle necking. Instead, coalescence occurred in a few frames with the small particle behaving in a liquid-like manner, once some activation barrier was overcome.

Figure 5b and c shows two frames from the video during particle coalescence. The entire coalescence process was completed within three frames of the video, which corresponds to ~0.1 s at a frame rate of 30 fps. It can be inferred from Fig. 5b and c that the coalescence in present case was preceded by an atomic flux that spreads out between the two particles, presumably on the substrate. This flow of atoms takes place in the region around the point of contact between the two particles indicated by lines in Fig. 5a. The dark contrast in the region bounded by the lines provides direct evidence of atomic flux between the particles. Note that this contrast appeared while the small particle remained completely spherical and in much stronger contrast, because it was much thicker. Presumably, the flux of atoms has nearly the same composition as the small particle average, although it is possible that the composition is somewhat different, as discussed previously. It would be extremely difficult to determine the flux composition experimentally in the TEM without significantly affecting the coalescence process.

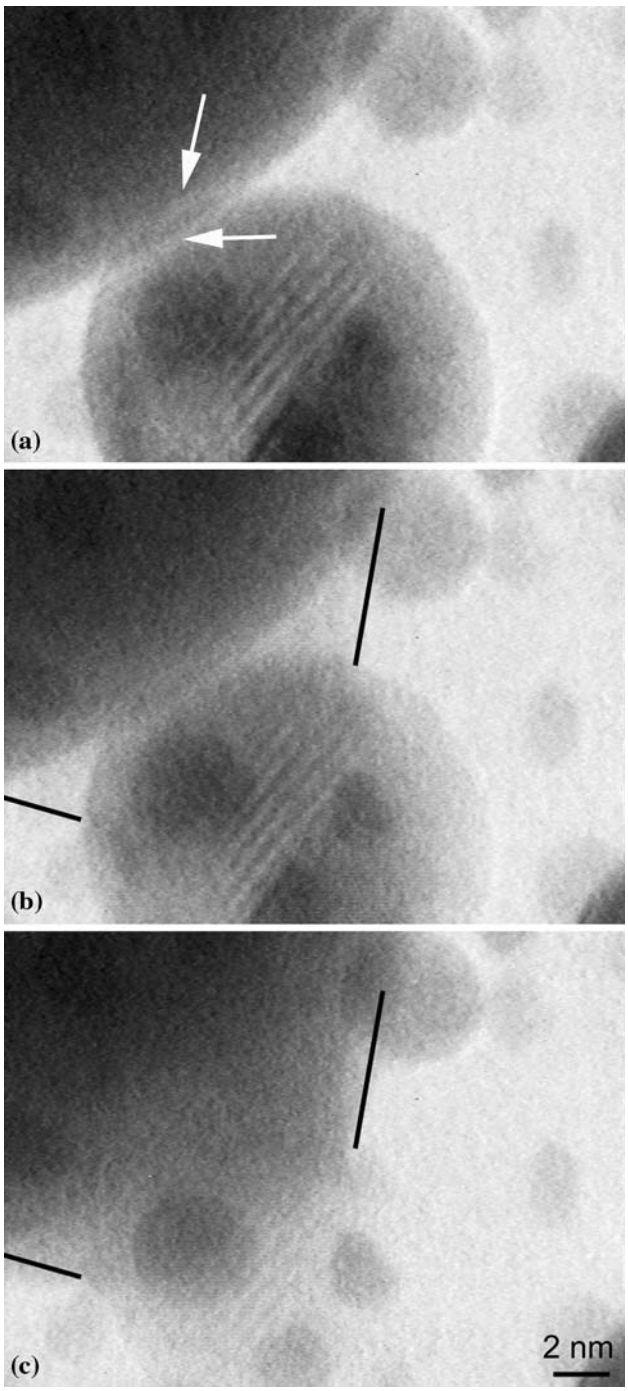

Fig. 5 **a** and **b** Shows particles in contact with each other before coalescence. The arrow in (**a**) indicates the presence of distinct surfaces of the two particles just before coalescence. In (**b**), the dark contrast within the region enclosed by dark lines indicates the presence of an atomic flux before coalescence, and **c** shows the liquid-like coalescence of small particles within 0.01 s

The small particle then moved to merge into the larger particle filling in this region three dimensionally, as evident by the darkened contrast in the image in Fig. 5c. During

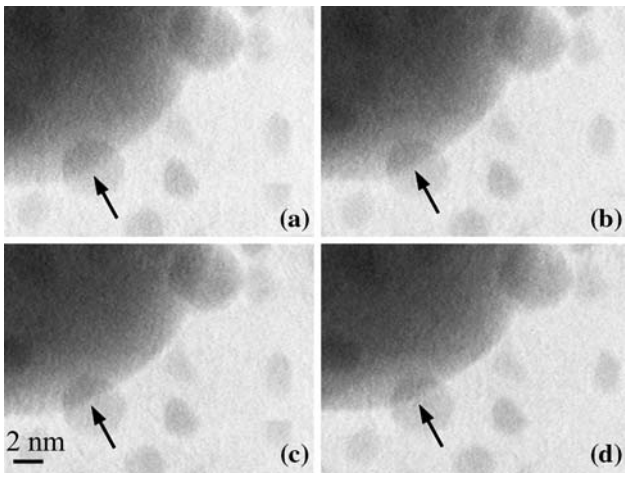

Fig. 6 **a–d** shows the receding edge of the large particle (marked by an arrow), indicating the redistribution of atoms. Note the position of the edge relative to the small stationary particle (under the arrow) on the opposite side of the support film

this process the small particle behaved more like a fluid than a solid body. In the next frame, shown in Fig. 6a, this mass of the small particle had become part of the larger particle. This newly acquired mass spread on the surface of the larger particle around the point of contact and did not appear to penetrate inside the larger particle. The mass was then redistributed around the larger particle and the particle edge receded back to its smoothly curved, original shape, as seen in Fig. 6b–d. Hence, it appeared that the mass associated with the small nanoparticle was initially spread locally on the contact surface of the large particle and then redistributed over the entire surface.

Conclusions

We analyzed the migration of a 15 nm Au–Cu nanoparticle on an amorphous-C substrate at a temperature of 300 °C using in situ TEM with point to point resolution as small as 0.2 nm. The key observations during the process of particle migration and coalescence are summarized as follows:

- The surface of the small particle was observed to fluctuate while approaching the large particle, demonstrating that collective atom process occurs along the particle periphery.
- The amplitude of fluctuation was largest for the edge closest to the large particle and also the direction of particle motion suggests that these fluctuations contribute toward particle motion.
- The size of the small particle decreased during the process of migration indicating that the particle was losing mass as it migrated toward the large particle. This indicates that an Ostwald ripening mechanism of coarsening was occurring, where atoms migrated from the small particle toward the large particle.
- Direct evidence of a diffusional flux from the small particle toward the large particle was observed before the coalescence process. The mass associated with the small particle flowed through the region defined by this diffusional flux during coalescence.
- Coalescence did not occur as soon as the particles came into contact, possibly due to an orientation difference between the particles. Coalescence eventually occurred for more than 15 s after the particles contacted, presumably as the orientation difference was overcome by deformation of the smaller particle. The actual coalescence process was completed in less than 0.1 s, although some mass continued to redistribute around the large particle for the next $\sim$0.15 s.

Acknowledgement This research was supported by the National Science Foundation under Grant DMR-0554792.

References

1. Datye AK (2003) J Catal 216:144
2. Lifshitz IM, Slyozov VV (1961) Phys Chem Solids 19:35
3. Voorhees PW (1985) J Stat Phys 38:231
4. Wynblatt P, Gjostein NA (1976) Acta Mater 24:1165
5. Zinke-Allmang M, Feldman LC, Grabow MH (1992) Surf Sci Rep 16:377
6. Morgenstern K, Rosenfeld G, Comsa G (1996) Phys Rev Lett 761:2113
7. Wen J-M, Chang S-L, Burnett JW et al (1994) Phys Rev Lett 73:2591
8. Morgenstern K, Rosenfeld G, Poelsema B et al (1995) Phys Rev Lett 74:2058
9. Reiss H (1968) J Appl Phys 39:5045
10. Bardotti L, Jensen P, Hoareau A et al (1995) Phys Rev Lett 74:4694
11. Ajayan PM, Marks LD (1988) Phys Rev Lett 60:585
12. Smith DJ, Petfordlong AK, Wallenberg LR et al (1986) Science 233:872
13. Jensen P, Clement A, Lewis LJ (2004) Comput Mater Sci 30:137
14. Yang W-C, Zeman M, Ade H et al (2003) Phys Rev Lett 90:136102
15. Sholl DS, Skodje RT (1996) Physica A 231:631
16. Zhu H, Averback RS (1996) Philos Mag Lett 73:27
17. Sinclair R, Itoh T, Chin R (2002) Microsc Microanal 8:288
18. Thune E, Carpene E, Sauthoff K, Seibt M, Reinke P (2005) J Appl Phys 98:034304
19. Chatterjee K, Howe JM, Johnson WC et al (2004) Acta Mater 52:2923
20. Lee JG, Mori H (2007) Solid State Phenom 127:135
21. Wallenberg R, Smith DJ, Bovin JO (1985) Ultramicroscopy 17(2):182
22. Jensen P (1999) Rev Mod Phys 71:1695
23. Wanner M, Werner R, Gerthsen D (2006) Surf Sci 600:632
24. Hwang HJ, Kwon O, Kang JW (2004) Solid State Commun 129:687
25. Lewis LJ, Jensen P, Combe N et al (2000) Phys Rev B 61:16084
26. Foiles SM, Baskes MI, Daw MS (1986) Phys Rev B 33:7983